



Nanosized $\text{LaCo}_{0.6}\text{Fe}_{0.4}\text{O}_3$ perovskites synthesized by citrate sol gel auto combustion method

Unikoth Megha^{1,*}, Karakat Shijina¹, George Varghese²

¹Department of Physics, University of Calicut, Kerala, 673635, India

²Kerala State Council for Science, Technology and Environment, Thiruvananthapuram, Kerala, 695004, India

Received 30 April 2014; Received in revised form 12 June 2014; Accepted 16 June 2014

Abstract

$\text{LaCo}_{0.6}\text{Fe}_{0.4}\text{O}_3$ (LCFO) nanopowder was synthesized from constituent metal nitrates, citric acid and ethylene glycol by citrate sol gel autocombustion method and calcined at different temperatures. The powders were characterized by X-ray diffraction (XRD), scanning electron microscopy (SEM), energy dispersive X-ray analysis (EDAX) and Fourier transform infrared spectra (FTIR), whereas dielectric properties were investigated with LCR-meter. The FTIR spectra, taken for the xerogel and the sample calcined at 1000 °C, confirm that the organic groups were removed during calcination and oxide structure was formed. The XRD result shows that LCFO has rhombohedral crystal structure with R-3C space group and forms single phase after calcination at 600 °C. The activation energy of crystallite growth, determined from the Arrhenius plot, was 17 ± 2 kJ/mol. Surface feature studies of the powders were obtained from SEM. At 1000 °C, dense microstructure with well-shaped grain boundaries was obtained and the average grain size was around 400 nm. EDAX confirms the elemental composition. Finally, from the dielectric studies, it was found that the dielectric constant (ϵ_r) as well as dielectric loss tangent ($\tan \delta$) decreases with increase in frequency.

Keywords: perovskites, lanthanum cobalt iron oxide, nanopowders, citrate sol gel auto combustion method

I. Introduction

Lanthanum-based perovskite type oxides are attractive materials due to their interesting optical, electric and magnetic properties as well as their potential applications. Their applications such as gas sensors, catalysts, thermoelectric materials, electrode materials in solid oxide fuel cells, provide a wide ranging interest in the synthesis and their structural analysis [1–4]. For achieving optimum performances and functional properties well defined microstructures are desirable, which in fact strongly depend on the method of synthesis [5].

Ideal perovskites have the ABO_3 stoichiometry (where A – rare earth, alkaline earth, alkali or large ions such as Pb^{+2} , Bi^{+3} and B – transition metal ion) and the ratio of bond length between A–O and B–O maintains a constant value which is equal to $\sqrt{2}$. The deviation from this is taken as the tolerance factor [6] and in terms of ionic radii, it assumes:

$$t = \frac{r_A + r_O}{\sqrt{2}(r_B + r_O)} \quad (1)$$

where r_A , r_B and r_O are the ionic radii of A and B cations and oxygen, respectively. The tolerance factor has a profound influence on the properties of substituted ABO_3 perovskites. Usually the metallic A-cation is co-ordinated by the neighbouring 12 oxygen ions, whereas the smaller B cation is co-ordinated by only 6 oxygen ions. Proper substitution of A or B can lead to oxygen deficiencies without altering the fundamental perovskite structures [7,8].

In the present work $\text{LaCo}_{0.6}\text{Fe}_{0.4}\text{O}_3$ perovskite nanopowder was synthesized by citrate sol gel auto combustion method. LaCoO_3 -based materials have interesting electrical and electro catalytic properties owing to their high electronic/ionic conductivity [9]. These materials have been prepared by many techniques which includes mechanical-synthesis [10], coprecipitation [11], solution combustion or thermal decomposition [12,13], solid-state reactions [14], Pechini [15], hydrothermal [16] and sol gel method. Many new methods or improvement of synthesis conditions have

* Corresponding author: tel: +91 90 4802 9595

fax: +91 49 4240 0269,

e-mail: meghaunikoth@gmail.com (U. Megha),

e-mail: gv@uoc.ac.in (G. Varghese)

been tried by the researchers as the properties of the end product strongly depend on the method of preparation technique used. Here we have used citrate sol gel auto combustion method, a modified Pechini method based on the polyesterification of citric acid and ethylene glycol for the synthesis of the title compound. The method involves relatively easy synthesis route when compared to the other conventional processes. Low operating temperature and control over the end stoichiometry are the main advantages of this technique.

Popa *et al.* [17,18] have synthesized perovskite - LaMeO_3 (Me – Mn, Co, Fe) compounds by the polymerizable complex method and elaborated its advantages. Compositional inhomogeneity, nonuniformity in particle size, high processing temperature, etc. are the disadvantages when the conventional mixed oxide routes are preferred for the synthesis. Perovskite nanopowders developed through chemical method have relatively good product uniformity and reliable reproducibility. By this method, it is possible to control the particle size and can reduce the agglomeration of nanoparticles. In citrate sol gel auto combustion route, at very low temperature excellent chemical homogeneity can be achieved. The nanopowders thus obtained have uniform particle size which allows sintering to give uniformly grained microstructures.

II. Experimental

$\text{LaCo}_{0.6}\text{Fe}_{0.4}\text{O}_3$ (LCFO) nanopowder was prepared by polymeric precursor method using $\text{La}(\text{NO}_3)_3 \times 6\text{H}_2\text{O}$, $\text{Co}(\text{NO}_3)_2 \times 6\text{H}_2\text{O}$, $\text{Fe}(\text{NO}_3)_3 \times 9\text{H}_2\text{O}$, citric acid, ethylene glycol (all Sigma Aldrich 99–99.99% purity), nitric acid and deionised water. The precursor solution was prepared by mixing metal nitrates, citric acid, nitric acid and deionised water. The solution was ultra-sonicated

for complete dissolution of metal cations in solution. The molar ratio of citric acid to the metal cation was 2 : 1. The solution was well stirred using magnetic stirrer and heated to about 60 °C. Ethylene glycol was added to the above solution in the molar ratio as 3 : 1 with citric acid. The resultant solution was heated in a hot plate to about 90 °C, transferred to water bath at 100 °C in order to form gel and finally to a hot mantle, having temperature up to 350 °C. The boiled solution undergone dehydration to form polymer complex, followed by decomposition with enormous swelling, produce foam and auto combustion, to form fine black powders. The precursor powder (xerogel) was well ground with an agate mortar and calcined at different temperatures ranging from 500 °C to 1000 °C for 6 h. Figure 1 shows the typical flow diagram of the preparation of compounds by citrate sol gel auto combustion method.

Phase confirmation and crystal structure of the compounds were determined by X-ray diffractometer (Rigaku Miniflex 600) with $\text{Cu K}\alpha$ radiation ($\lambda = 0.154$ nm), at 40 kV and 15 mA, at room temperature in the diffraction angle range 20–80° with scan rate of 2° per minute and step of 0.02°. The lattice parameters and the average crystallite size were calculated using PDXL-software. The crystallite size was also compared with the values obtained using Debye-Scherrer formula, $D = 0.9 \cdot \lambda / (\beta \cdot \cos \theta)$ where λ is X-ray wavelength and β is peak width at half maximum. Morphology of the powder and the elemental composition were recorded by scanning electron microscope (SEM, JEOL 5600 LV, Tokyo, Japan). FTIR transmission spectra in the region from 400–4000 cm^{-1} were measured using Perkin-Elmer 2000 FTIR spectrometer. The sample was taken in pellet form in KBr matrix for measurement. The calcined powders (1000 °C), mixed with PVA, were used for the preparation of the cylindrical pellet, which were

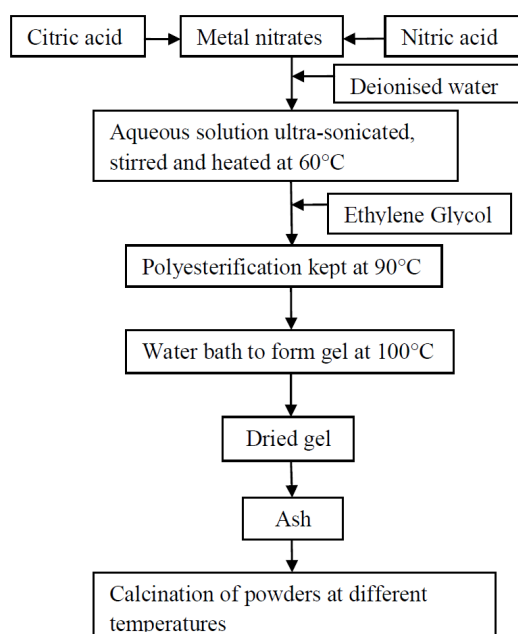


Figure 1. Flow chart for the compound preparation by citrate sol gel auto combustion method

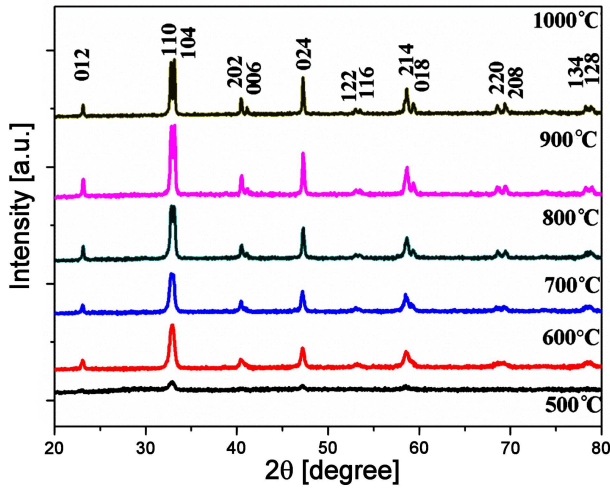


Figure 2. XRD of precursor powders calcined at different temperatures

Table 1. Lattice parameters (a and c) and the average crystallite size (D) of LCFO powders calcined at different temperatures, obtained using PDXL software

Calcined temperature [°C]	Lattice parameters		D [nm]
	a [Å]	c [Å]	
600	5.523	13.128	14.2
700	5.473	13.227	15.3
800	5.475	13.242	22.7
900	5.479	13.204	34.4
1000	5.473	13.186	42.6

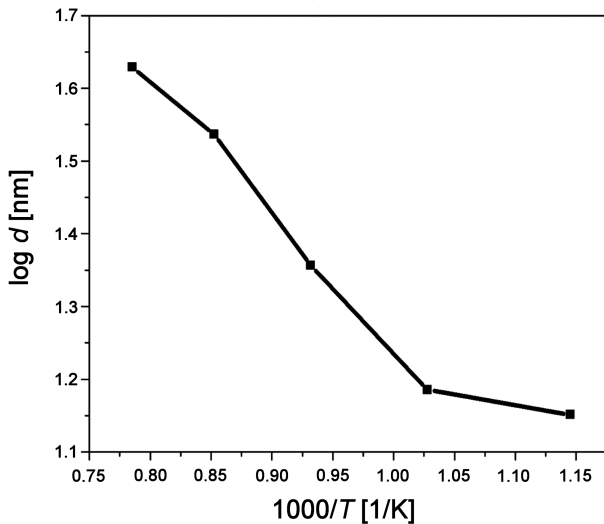


Figure 3. Crystallite size (d) of calcined powders versus temperature ($1/T$) in Arrhenius plot

then fired at 350 °C to reduce the influence of the polymer matrix, while measuring the dielectric properties. The dielectric measurements at room temperature were carried out by using LCR Hi TESTER 3532-50 meter in the frequency range 100 Hz–1 MHz.

III. Results and discussion

The XRD patterns of the precursor powder calcined at different temperature ranging from 500 °C to 1000 °C for 6 h were shown in Fig. 2. Single phase perovskite structure was obtained after calcination at 600 °C. $\text{LaCo}_{0.6}\text{Fe}_{0.4}\text{O}_3$ has trigonal crystal structure, i.e. $a = b \neq c$ and $\alpha = \beta = 90^\circ$, $\gamma = 120^\circ$ with $R\text{-}3C$ space group (ICDD-01-074-9368). The lattice parameters and the average crystallite size, calculated using PDXL-software at different temperatures, were tabulated in Table 1. It was observed that the crystallite size increases with temperature which may be due to the growth of particle size. The activation energy for crystallite growth was determined using Arrhenius equation for rate constant:

$$k = A \cdot e^{-\frac{E_a}{RT}} \quad (2)$$

where A is a constant related to the number, orientation and frequency of collisions occurring between the particles in the reaction, E_a is activation energy, R is universal gas constant and T is the absolute temperature. The activation energy of 17 ± 2 kJ/mol was calculated from the plot crystallite size versus $1/T$ (Fig. 3) [19]. The Arrhenius plot, more or less appears straight, up to temperature 900 °C, and deviates from its normal nature when the calcination temperature increased above 900 °C. The respective behaviour changes can be notice in SEM as well as FTIR spectra of the samples calcined at 1000 °C.

The scanning electron micrographs of the samples, shown in Fig. 4, reveal that the calcination has increased the particle size, as well as changed morphology. As calcination temperature increases, the particles become tightly stacked and their shape changes from lenticular to spherical which is attributed to the grain growth phenomenon. The formation of sufficiently large dense microstructures appears around 1000 °C, having grain size ~ 400 nm. From EDAX, the elemental composition was determined and the percentage of elements present was tabulated in Table 2.

Table 2. The percentage of elements present in the sample

Element	Elemental composition	
	[wt.%]	[at.%]
O	17.06	56.22
Fe	9.92	9.36
Co	13.03	11.65
La	59.99	22.77
Total	100.00	

The infrared spectra in the range 400–4000 cm^{-1} of the LCFO precursor powder and the powder calcined at 1000 °C for 6 h are presented in Fig. 5. It can be seen that many organic groups are present in the precursor powder. The broad band at 3400 cm^{-1} is assigned to stretching vibration of OH group [20]. The band due to asymmetric stretching vibrations of $-\text{CH}_2$ groups can be noticed at 2923 cm^{-1} . The absorption

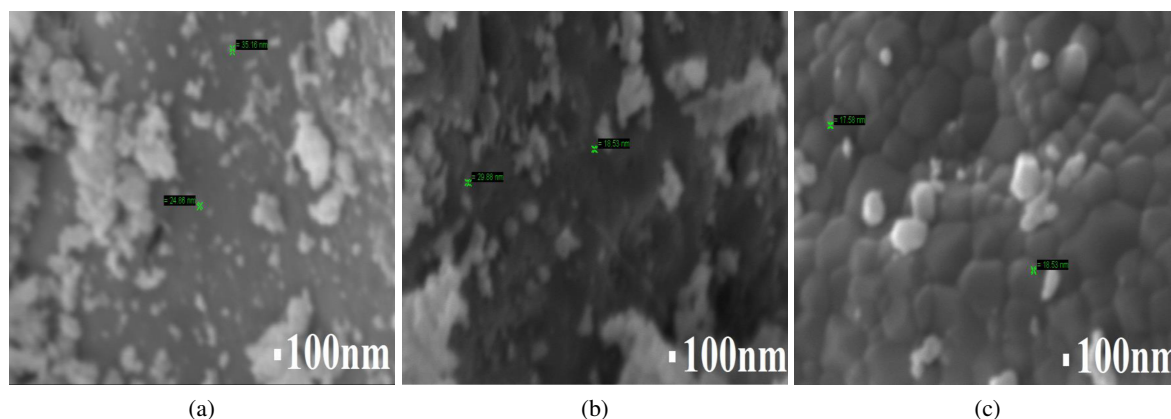


Figure 4. SEM micrographs of precursor powders calcined for 6 h at: a) 600 °C, b) 800 °C and c) 1000 °C

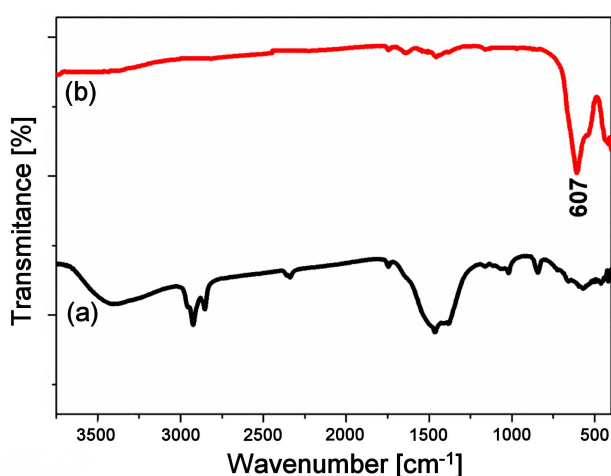


Figure 5. IR spectra of LCFO: a) precursor powder and b) powder calcined at 1000 °C for 6 h

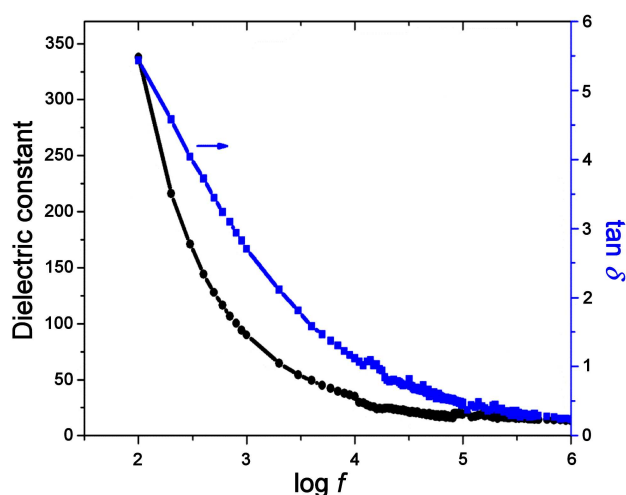


Figure 6. Variation of dielectric constant and loss coefficient with frequency (f) at room temperature

band at 2853 cm^{-1} is due to the symmetric stretching vibration of $-\text{CH}_2$ groups [21]. The absorption band of $-\text{C}=\text{O}$ stretching is at 1746 cm^{-1} [22]. The characteristic band around 1636 cm^{-1} is assigned for $\text{C}=\text{O}$ stretching in carboxyl or amide groups. The bands at 1465 cm^{-1}

correspond to $-\text{CH}_2$ bend [23]. At 1019 cm^{-1} there is $\text{C}-\text{N}$ stretching band [24]. The band 842 cm^{-1} is due to $\text{C}-\text{H}$ bending [25]. The bands around 600 cm^{-1} and 480 cm^{-1} are characteristic metal–oxygen bond. The absorption peak at 571 cm^{-1} is assigned for $\text{Fe}-\text{O}$ bond. It was observed that the organic functional group vanishes at high temperature due to the breakage of organic bonds.

The dielectric constant is calculated using the equation: $\epsilon_r = C \cdot d / (\epsilon_0 \cdot A)$ (where C is capacitance, d is thickness, ϵ_0 is permittivity of free space and A is area of cross section of pellet). The density of the LCFO pellet obtained using Archimedes method was 5.23 g/cm^3 . It was observed from Fig. 6 that the dielectric constant and dielectric loss tangent ($\tan \delta$) decreases with frequency, which is a general ferroelectric behaviour [26]. At lower frequency, the total dielectric constant will be due to the combined electronic, atomic/ionic, dipolar and interfacial/surface polarizations. But, as the frequency increases the interfacial, dipolar and atomic/ionic polarisation becomes zero and the electronic polarisation alone influences the dielectric constant. At higher frequency, the value of dielectric constant will be small and polarons cannot be able to follow the electric field, which results in frequency independent polarisation [27–29].

IV. Conclusions

$\text{LaCo}_{0.6}\text{Fe}_{0.4}\text{O}_3$ perovskite nanopowder was successfully synthesised by citrate sol gel auto combustion method by using citric acid and ethylene glycol. Phase pure $\text{LaCo}_{0.6}\text{Fe}_{0.4}\text{O}_3$ powder with rhombohedral crystal structure was obtained by adequate thermal treatment at 600 °C . XRD confirms the formation of perovskite structure and the average particle size confirms their nanosized nature. The activation energy for crystallite growth calculated from the Arrhenius plot was $17 \pm 2\text{ kJ/mol}$. The sample loses all its organic components at 1000 °C . As the calcination temperature goes above 900 °C , changes have been noticed in structure, morphology, optical spectra as well as in the behaviour

of rate constant with temperature. Scanning electron micrograph showed the formation of dense microstructure at 1000 °C with average grain size around 400 nm. In the frequency range from 100 Hz–1 MHz at room temperature sample behaves like a good dielectric material.

Acknowledgement: Two of the authors acknowledge UGC, Govt. of India, for the BSR Fellowship. The authors express sincere gratitude to S. Sindhu and Jabeen Fathima, Department of Nanoscience and Technology and P.P. Pradyumn, Department of Physics, of the University of Calicut for experimental support and for valuable suggestions rendered during the study.

References

1. C. Feng, S. Ruan, J. Li, B. Zou, J. Luo, W. Chen, W. Dong, F. Wu, "Ethanol sensing properties of $\text{LaCo}_x\text{Fe}_{1-x}\text{O}_3$ nanoparticles: Effects of calcination temperature, Co-doping, and carbon nanotube - treatment", *Sensors Actuators B*, **155** (2011) 232–238.
2. F. Bin, C. Song, G. Lv, J. Song, C. Gong, Q. Huang, " $\text{La}_{1-x}\text{K}_x\text{CoO}_3$ and $\text{LaCo}_{1-y}\text{Fe}_y\text{O}_3$ perovskite oxides: Preparation, characterization, and catalytic performance in the simultaneous removal of NO_x and diesel soot", *Ind. Eng. Chem. Res.*, **50** (2011) 6660–6667.
3. V. Vulchev, L. Vassilev, S. Harizanova, M. Khristov, E. Zhecheva, R. Stoyanova, "Improving of the thermoelectric efficiency of LaCoO_3 by double substitution with nickel and iron", *J. Phys. Chem. C*, **116** (2012) 13507–13515.
4. S. Ghosh, S. Dasgupta, "Synthesis, characterization and properties of nanocrystalline perovskite cathode materials", *Mater. Sci. - Poland*, **28** [2] (2010) 427–438.
5. M. Popa, L. Hong, M. Kakihana, "Nanopowders of LaMeO_3 perovskites obtained by a solution-based ceramic processing technique", *Physica B*, **327** (2003) 233–236.
6. P.M. Woodward, "Octahedral tilting in perovskites II. Structure stabilizing forces", *Acta Crystall. B*, **53** (1997) 44–66.
7. C. Singh, M. Rakesh, "Preparation and characterization of nickel doped, A and B site LaCoO_3 perovskites", *Indian J. Eng. Mater. Sci.*, **16** (2009) 288–290.
8. D.S. Melo, E.P. Marinho, L.B. Soledade, D.A. Melo, S.G. Lima, E. Longo, I.M. Garcia Santos, A.G. Souza, "Lanthanum-based perovskites obtained by the polymeric precursor method", *J Mater. Sci.*, **43** (2008) 551–556.
9. F.M. Figueiredo, F.M.B. Marques, J.R. Frade, "Electrochemical permeability of $\text{La}_{1-x}\text{Sr}_x\text{CoO}_{3-\delta}$ materials", *Solid State Ionics*, **111** (1998) 273–281.
10. V. Szabo, M. Bassir, A. Van Neste, S. Kaliaguine, "Perovskite-type oxides synthesized by reactive grinding Part II: Catalytic properties of $\text{LaCo}_{(1-x)}\text{Fe}_x\text{O}_3$ in VOC oxidation", *Appl. Catal. B Environ.*, **37** (2002) 175–180.
11. X. Ge, Y. Liu, X. Liu, "Preparation and gas-sensitive properties of $\text{LaFe}_{1-y}\text{Co}_y\text{O}_3$ semiconducting materials", *Sensors Actuators B*, **79** (2001) 171–174.
12. N.P. Bansal, Z. Zhong, "Combustion synthesis of $\text{Sm}_{0.5}\text{Sr}_{0.5}\text{CoO}_{3-x}$ and $\text{La}_{0.6}\text{Sr}_{0.4}\text{CoO}_{3-x}$ nanopowders for solid oxide fuel cell cathodes", *J. Power Sources*, **158** (2006) 148–153.
13. D. Berger, C. Matei, F. Papa, G. Voicu, V. Fruth, Prog, "Pure and doped lanthanum cobaltites obtained by combustion method", *Solid State Chem.*, **35** (2007) 183–191.
14. S. Royer, A. Van Neste, R. Davidson, S. McIntyre, S. Kaliaguine, "Methane oxidation over nanocrystalline $\text{LaCo}_{1-x}\text{Fe}_x\text{O}_3$: Resistance to SO_2 poisoning", *Ind. Eng. Chem. Res.*, **43** (2004) 5670–5680.
15. M.P. Pechini, "Method of preparing lead and alkaline earth titanates and niobates and coating method using the same to form a capacitor", U.S. Patent No. 3 330 697, 1967.
16. W. Zheng, R. Liu, D. Peng, G. Meng, "Hydrothermal synthesis of LaFeO_3 under carbonate-containing medium", *Mater. Lett.*, **43** (2000) 19–22.
17. M. Popa, M. Kakihana, "Synthesis of lanthanum cobaltite (LaCoO_3) by the polymerizable complex route", *Solid State Ionics*, **151** (2002) 251–257.
18. M. Popa, J. Frantti, M. Kakihana, "Characterization of LaMeO_3 (Me: Mn, Co, Fe) perovskite powders obtained by polymerizable complex method", *Solid State Ionics*, **154-155** (2002) 135–141.
19. M. Popa, J. Frantti, M. Kakihana, "Lanthanum ferrite LaFeO_{3+d} nanopowders obtained by the polymerizable complex method", *Solid State Ionics*, **154-155** (2002) 437–445.
20. M.A. Farrukh, C.M. Simonescu, *Advanced Aspects of Spectroscopy*, InTech, Croatia, 2012.
21. S. Feng, Z. Ren, Y. Wei, B. Jiang, Y. Liu, L. Zhang, W. Zhang, H. Fu, "Synthesis and application of hollow magnetic graphitic carbon microspheres with/without TiO_2 nanoparticle layer on the surface", *Chem. Commun.*, **46** (2010) 6276–6278.
22. V. Kampars, S. Kronberga, "Iodine values estimation of vegetable oils by FTIR spectroscopy", *Pol. J. Food Nutr. Sci.*, **12/53** (2003) 45–47.
23. G.V. Venkataramana, J.K. Kumar, A.G. Prasad, P. Karim, "Fourier transform infrared spectroscopic study on liver of freshwater fish *Oreochromis Mossambicus*", *Romanian J. Biophys.*, **20** (2010) 315–322.
24. S. Annapoorani, V.R. Parameswaran, "Studies on complexes of 1,2-Bis-(8-quinoy) ethane with some bivalent metal ions", *Asian J. Chem.*, **11** (1999) 763–766.
25. B.H. Boo, "Infrared and Raman spectroscopy of diphenylsilane. Vibrational assignment by Hartree-Fock and density-functional theory calculations", *J.*

- Korean Phys. Soc.*, **59** (2011) 3205–3209.
26. T. Huang, Y. Chang, G. Chen, C. Chung, Y. Chang, “The structural characterization and dielectric properties of the $\text{La}_{1-x}\text{K}_x\text{Co}_{1-x}\text{Nb}_x\text{O}_3$ ($x = 0-1$) system dielectric science and materials”, *J. Electrochem. Soc.*, **154** (2007) 244–250.
27. K. Jawahar, R.N.P. Choudhary, “Structural and dielectric properties of $\text{LaBi}_2\text{Fe}_5\text{O}_{12}$ ”, *Indian J. Eng. Mater. Sci.*, **15** (2008) 203–206.
28. S. Acharya, P.K. Chakrabarti, “Some interesting observations on the magnetic and electric properties of Al^{+3} doped lanthanum orthoferrite ($\text{La}_{0.5}\text{Al}_{0.5}\text{FeO}_3$)”, *Solid State Commun.*, **150** (2010) 1234–1237.
29. W. Haron, T. Thaweechai, W. Wattanathana, A. Laobuthee, H. Manaspiya, C. Veranitisagul, N. Koonsaeng, “Structural characteristics and dielectric properties of $\text{La}_{1-x}\text{Co}_x\text{FeO}_3$ and $\text{LaFe}_{1-x}\text{Co}_x\text{O}_3$ synthesized via metal organic complexes”, *Energy Procedia*, **34** (2013) 791–800.